Copolymerization of Poly(1-naphthylamine) with Aniline and *o*-Toluidine

Ufana Riaz, Reshma Jahan, Sharif Ahmad, S. M. Ashraf

Materials Research Laboratory, Department of Chemistry, Jamia Millia Islamia, New Delhi 110025, India

Received 12 September 2007; accepted 8 December 2007
DOI 10.1002/app.27922
Published online 20 February 2008 in Wiley InterScience (www.interscience.wiley.com).

ABSTRACT: The commercial use of polyaniline has been impeded by its intractable nature and insolubility. The use of substituted polyaniline has been attempted mainly to increase the processibility of polyaniline, but this approach usually results in the lowering of the conductivity. This study reports the synthesis of poly(1-naphthylamine), a fused ring derivative of polyaniline, and its copolymers with aniline and *o*-toluidine via a chemical polymerization method. Spectral, thermal, morphological, and conductivity studies were carried out to elucidate the influence of the incorporation of aniline and *o*-toluidine units into poly(1-naphthylamine). © 2008 Wiley Periodicals, Inc. J Appl Polym Sci 108: 2604–2610, 2008

Key words: conducting polymers; copolymerization; morphology; nanotechnology; thermal properties

INTRODUCTION

In recent years, extensive efforts have been devoted to developing newer techniques to synthesize polyaniline (PANI) with improved mechanical properties and high conductivity. Common methods adopted to enhance the processibility of PANI include the synthesis of PANI blends and composites with excellent electrical properties coupled with good environmental stability.[1,2] The solubility of PANI can also be improved by the copolymerization of a derivative of aniline and particularly by the choice of the substituents, which have a solubilizing effect. This has been established as a convenient method for the preparation of novel conducting materials with desired properties superior to those of individual homopolymers. The substituents used to modify the solubility of PANI range from alkyl[3] and alkoxy[4] groups to phase-substituted PANIs. Pioneering work was conducted by Wei and coworkers,[5,6] who showed that aniline could be copolymerized with *o*-toluidine to control conductivity in a broad range. Bergeron and Dao[7] reported the electrosynthesis of a copolymer of aniline and *N*-butyl aniline with good conductivity and solubility in common organic solvents. Successful copolymerizations of aniline with *N*-methylaniline,[8] 3-aminophenyl boric acid,[9] and *o*-aminobenzonitrile[10] have also been reported.

Correspondence to: S. M. Ashraf (smashraf_jmi@yahoo.co.in).

Contract grant sponsor: Council of Scientific and Industrial Research (CSIR); contract grant number: 01/1953/04/EMR-II.

Journal of Applied Polymer Science, Vol. 108, 2604–2610 (2008)

Poly(1-naphthylamine) (PNA) is an aromatic polymer that has attracted much less attention than polypyrrole, PANI, and polythiophene.[11,12] However, being an aniline derivative, it should possess electrical and optical properties similar to those of the aforementioned polymers with higher processibility and better performance due to the low band-gap energy.[12–14] Many reports are available on the preparation of PNA via chemical[12] and electrochemical[13,14] methods. The catalytic activities of PNA complexes with Ni(II) and Co(II) ions have also been reported,[15] and PNA-modified electrodes have been used as biosensors for NADH/NAD redox systems.[16]

The effect of copolymerization on the properties of PNA has not yet been studied, particularly with nanoscale synthesis. Our aim is to investigate the effect of the copolymerization of PNA with the well-known conducting polymers PANI and poly(*o*-toluidine). With the further aim of enhancing the processibility and conductivity, the synthesis of PNA and its copolymers with aniline and *o*-toluidine has been carried out by the inverse emulsion polymerization method in the presence of a cationic surfactant. With the aim of obtaining a suitable solubilizing comonomer to enhance the processibility and conductivity, this work reports the synthesis of PNA and its copolymers with aniline and *o*-toluidine by the inverse emulsion polymerization method in the presence of a cationic surfactant. It has been reported that chemical polymerization in well-organized micelles of surfactants such as sodium dodecyl sulfate, dodecyl benzene sulfonic acid, and camphor sulfonic acid accelerates polymerization and helps in obtaining nanoscale particles.[17] Inverse emulsion polymerization increases the interaction between the

oxidant, dopant, and monomers because the reaction occurs in a large number of loci dispersed in a continuous phase providing a larger surface area for polymerization.[17] The synthesized polymer and copolymers have been characterized with Fourier transform infrared (FTIR), ultraviolet–visible (UV–vis), thermogravimetric analysis (TGA), and transmission electron microscopy (TEM) techniques. The effect of copolymerization on the morphological, thermal, and conductivity characteristics of the resulting copolymers has been analyzed.

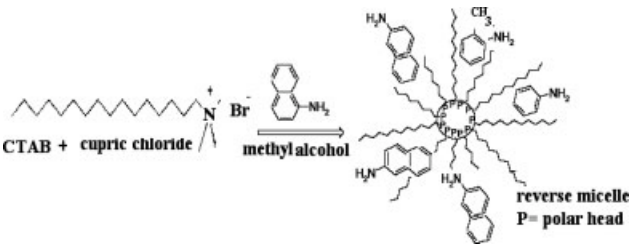

Scheme 1 Reverse micelle polymerization of PNA and its copolymers.

EXPERIMENTAL

Materials required

Monomers

1-Naphthylamine (NPA; $C_{10}H_9N$; Loba Chemie, Mumbai, India; molecular weight = 143.19, mp = 47–50°C) was purified before use. The monomer was sublimed at 120°C and recrystallized with ethanol (EtOH). Aniline (C_6H_7N; Merck, Mumbai, India; molecular weight = 93.13, bp = 112°C) and *o*-toluidine ($C_7H_{10}N$; Merck; molecular weight = 108, bp = 120°C) were double-distilled under reduced pressure and stored in a refrigerator before use. The initiator, cupric chloride ($CuCl_2{\cdot}2H_2O$; Qualigen, Mumbai, India; molecular weight = 170; assay, 99% minimum, 0.05% sulfate, and 0.05% iron), was analytical-grade and was used without further purification. The surfactant was *N*-cetyl-*N*,*N*,*N*-trimethyl ammonium bromide (CTAB; $C_{19}H_{42}BrN$; Loba Chemie; molecular weight = 364.46; minimum assay, iodometric, 0.001% heavy metal platinum, 0.1% sulfated ash, and 0.001% iron). The solvent was methanol (MeOH; CH_3OH; Merck; molecular weight = 32; minimum assay, impurities 0.001% EtOH and 0.01% nonvolatile matter).

Synthesis of PNA and its copolymers with aniline and *o*-toluidine

In a typical experiment, 0.303 g of cupric chloride (0.5*M*) was added to a 100-mL, round-bottom flask containing 35 mL of methyl alcohol. The mixture was kept under mechanical stirring. CTAB (2.2 g) and naphthylamine monomer (0.232 g) were added simultaneously to the aforementioned mixture and were followed by the addition of 15 mL of water to form an inverse emulsion (Scheme 1). Here NPA–CTAB in water formed the dispersed phase, whereas cupric chloride in methyl alcohol formed the continuous phase. The reaction mixture gradually turned purple in 2.5 h, and the stirring was continued for 28 h at room temperature. At the end of the reaction, the purple-black product was isolated from the reaction mixture by filtration on a glass frit and was washed thoroughly with distilled water, and acetone was used to remove the surfactant and other impurities. Further purification of the polymer was performed in a Soxhlet fashion with MeOH for a period of 16 h to remove oligomeric fractions and other impurities. The copolymers poly(naphthylamine-*co*-aniline) (PNA-*co*-PANI) and poly(naphthylamine-*co*-*o*-toluidine) (PNA-*co*-POT) were synthesized with the aforementioned procedure with 1:1 monomer feed ratios of NPA to *o*-toluidine and NPA to aniline. The samples were dedoped by washing with a 5% ammonium hydroxide solution. The powders of the homopolymers and copolymers were then dried *in vacuo* at 50°C for 72 h.

Characterization

Spectral analysis

FTIR spectra of the powdered polymers and copolymers were taken in the form of KBr pellets on a PerkinElmer 1750 FTIR spectrophotometer (PerkinElmer Cetus Instruments, Norwalk, CT). UV–vis spectra were taken on a PerkinElmer Lambda EZ-221 for the solutions of the polymer and copolymers prepared in dimethyl sulfoxide (DMSO).

Thermal analysis

TGA was recorded on a TGA51 thermogravimetric analyzer from T.A. Instruments (New Castle, DE) in a nitrogen atmosphere at a heating rate of 10°C/min.

Morphological analysis

Transmission electron micrographs were taken on a Morgagni (Tokyo, Japan) 268-D FEI transmission electron microscope. The samples were prepared by the deposition of a drop of a well-diluted polymer and copolymer suspension onto a carbon (1 0 0)-coated copper grid and dried in an oven at 55°C for 2 h. X-ray diffractograms were recorded in the powdered form on a Philips PW3710 X-ray diffractometer (Midland, Canada) with Cu Kα radiation.

Conductivity measurements

Samples were doped in a desiccator for 24 h. Hydrochloric acid vapor and iodine were used for doping. Pressed pellets of the polymer and copolymer powders were obtained by the subjection of the powders to a pressure of 50 kN. Conductivity measurements were performed by the standard four-probe method with a Keithley (Cleveland, OH) DMM 2001 and an EG&G Princeton Applied Research model 362 potentiostat as a current source. The error in the resistance measurements under these conditions was less than 2%.

RESULTS AND DISCUSSION

Solubility of PNA and its copolymers

The PNA powder showed a dark purple color, whereas PNA-*co*-PANI and PNA-*co*-POT were bluish-black. The yields of PNA, PNA-*co*-PANI, and PNA-*co*-POT were comparable, being 65, 60, and 70%, respectively. This confirms that the presence of the fused aromatic ring of PNA exhibited no steric hindrance during copolymerization. The homopolymer PNA was soluble in most organic solvents, including tetrahydrofuran (THF), DMSO, dimethylformamide (DMF), chloroform ($CHCl_3$), CH_2Cl_2, EtOH, and MeOH, whereas the copolymers were mainly soluble in *N*-methylpyrrolidone (NMP), DMF, and DMSO (Table I). The lower solubility of the copolymers could be attributed to their morphology, which is discussed in the following section.

Spectral analysis

FTIR spectra

The FTIR spectrum of PNA [Fig. 1(a)] shows a broad N—H stretching vibration peak centered at 3370 cm^{-1} for a secondary amine. The broadness of the peak indicates polymer formation. The peaks at 1514 and 1467 cm^{-1} can be assigned to the C=C skeletal vibrations [ν(C=C)], whereas the absorption peak at

TABLE I
Solubility of PNA and Its Copolymers

PNA-*co*-POT	PNA-*co*-PANI	PNA	Solvent
IS	IS	IS	H_2O
SS	SS	S	EtOH
SS	SS	S	MeOH
IS	IS	S	$CHCl_3$
IS	IS	SS	Acetone
IS	IS	S	Methylene chloride
S	S	S	THF
S	S	S	DMSO
S	S	S	DMF
S	S	S	NMP

S = soluble; SS = sparingly soluble; IS = insoluble.

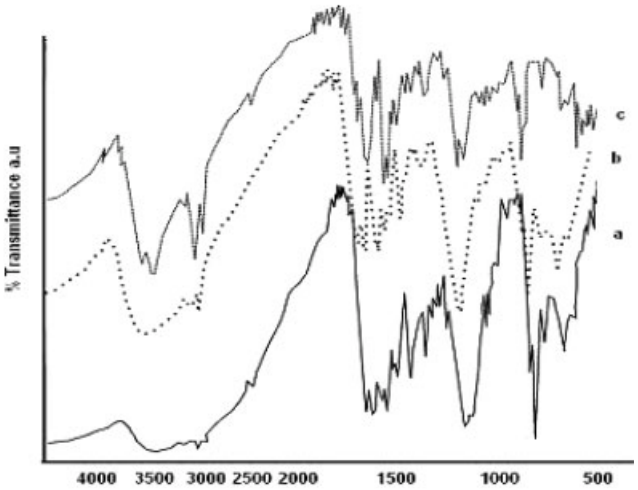

Figure 1 FTIR spectra of (a) PNA, (b) PNA-*co*-PANI, and (c) PNA-*co*-POT.

1617 cm^{-1} can be correlated to the imine stretching mode.[12] The peak at 1578 cm^{-1} can be assigned to the NH deformation vibration.[18] The bands at 1329, 1286, and 1245 cm^{-1} are due to the CN stretching vibration. A pronounced peak at 1121 cm^{-1} is assigned to the benzenoid–NH–benzenoid and benzenoid–NH–quinonoid vibration modes.[18] The aforementioned analysis shows the presence of imine (C=N) and secondary amine linkages in PNA and hence the presence of benzenoid and quinonoid units. It also shows head-to-tail CN coupling in the polymer. The peaks between 700 and 900 cm^{-1} due to the C—H deformation mode have been used to establish the position of coupling between two naphthylamine units.[18] The coupling of the 1,4- and 1,5-types are most favorable, whereas the 1,7-type can also be observed.[18] The peaks at 769 and 842 cm^{-1} are consistent with 1,4-coupling with two and four vicinal hydrogens on the two aromatic rings of the naphthylamine.[18] The peak at 792 cm^{-1} is attributed to 1,5-coupling with three vicinal hydrogens on each benzene ring of NPA.[12,18] The highly pronounced peak at 792 cm^{-1} also shows a larger number of 1,5-coupled units. The polymer therefore is a mixture of 1,4- and 1,5-coupled naphthylamine units.

The spectrum of PNA-*co*-PANI [Fig. 1(b)] exhibits a shift in the CN peaks from 1286 to 1289 cm^{-1}. The presence of pronounced CN, NH, B—NH—B, and B—NH—Q peaks indicates the presence of additional benzenoid and quinonoid rings, thereby confirming the formation of a copolymer of naphthylamine with aniline.[19] The broadness of the NH vibration peak occurs presumably because of hydrogen bonding between the chains of the polymers through NH of aniline with the fused aromatic ring of NPA.

The spectrum of PNA-*co*-POT [Fig. 1(c)] shows a shift of 32 cm^{-1} in the NH vibration peak that appears at 3338 cm^{-1}, whereas a new NH vibration

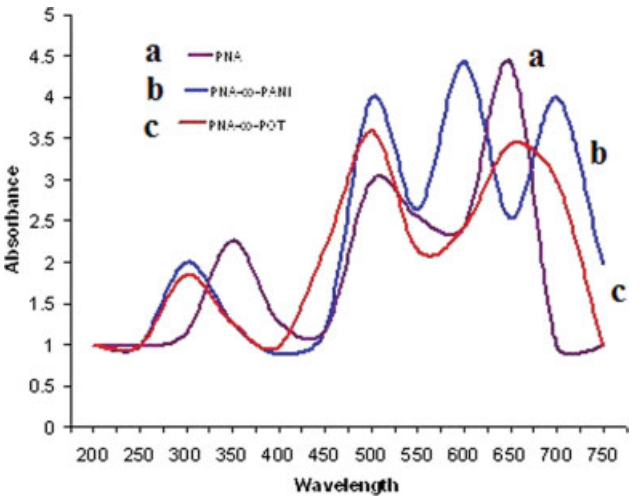

Figure 2 UV–vis spectra of PNA and its copolymers. [Color figure can be viewed in the online issue, which is available at www.interscience.wiley.com.]

peak can be observed at 3499 cm^{-1}, indicating that no hydrogen bonding takes place in this copolymer. Multiple peaks appear between 1700 and 1200 cm^{-1} that can be correlated to the C=C skeletal vibrations and imine stretching modes. A major shift in the CN vibration peak is observed from 1286 to 1208 cm^{-1}. The presence of additional B—NH—B and B—NH—Q vibration peaks at 1153 cm^{-1} confirms the copolymerization of *o*-toluidine with PNA. The B—NH—B peak observed at 1121 cm^{-1} in the case of pristine PNA shows a shift of 6 cm^{-1} toward a lower frequency having much lower intensity because of steric hindrance caused by a methyl substituent of *o*-toluidine that results in a decrease in the conjugation length of this polymer. Similar observations were recorded from the UV–vis spectra of the same.

UV–vis spectra

The UV–vis spectrum of PNA in DMSO (Fig. 2) consists of absorption bands at 350, 510, and 650 nm. The first peak can be attributed to π–π* transitions in the benzenoid rings, the second peak can be attributed to the excitonic transition of the quinonoid rings,[12] and the third peak can be correlated to the polaronic transition.[12] The UV–vis spectrum of PNA-*co*-PANI in DMSO (Fig. 2) shows absorption maxima at 300, 500, 600, and 720 nm. The 500- and 600-nm peaks are attributed to excitonic transitions in PNA and PANI units, respectively, in the copolymer.[20,21] The pronounced 720-nm peak in the spectrum of PNA-*co*-PANI arises from polaronic transitions in PANI (an emeraldine salt state with an enhanced conjugation length of the copolymer backbone). Several authors have correlated this peak to the aforementioned transition in PANI.[22–24] The spectrum of PNA-*co*-POT shows absorption maxima at 300 and 500 nm, a suppressed peak at 580 nm, and a broad peak at 650 nm. The correlation of the peaks is the same as that in the case of PNA-*co*-PANI. The 650-nm peak is broad and is of low intensity. The polaronic transition in this case occurs at a lower wavelength because of lower conjugation. This also shows a compact coil structure of the copolymer due to the presence of methyl groups of *o*-toluidine.

From these observations, it can be inferred that the shifting of the polaronic transition peaks in the UV spectra depends on the nature of the comonomer and the types of substituents present on the polymer backbone. The hypsochromic shift of the 350-nm band in the copolymers implies an increase in the torsional strain in the chain. The difference in the absorption maxima of the polaronic transition in the two copolymers shows changes in the chain length and extent of conjugation.[25,26] The hypsochromic shift in the polaronic transition in the case of PNA-*co*-POT compared with PNA-*co*-PANI results from a more coiled (compact) or rigid chain structure of the former due to the presence of a bulky methyl group on the benzene ring.[17,19]

X-ray analysis

The X-ray diffractogram of PNA [Fig. 3(a)] shows a prominent semicrystalline peak centered at 2θ = 19.00°, suggesting the ordered structure of the homopolymers. The diffractogram of the copolymer PNA-*co*-PANI [Fig. 3(c)] shows a broad hump centered at 18.00°, whereas the diffractogram of PNA-*co*-POT [Fig. 3(b)] shows a pronounced high-angle peak at 25.23° superposed on a broad hump that indicates a broadly amorphous structure. X-ray diffractograms of the copolymers show broadening of the peaks, which indicates that copolymers have an amorphous nature, whereas PNA is semicrystalline. The *d*-spac-

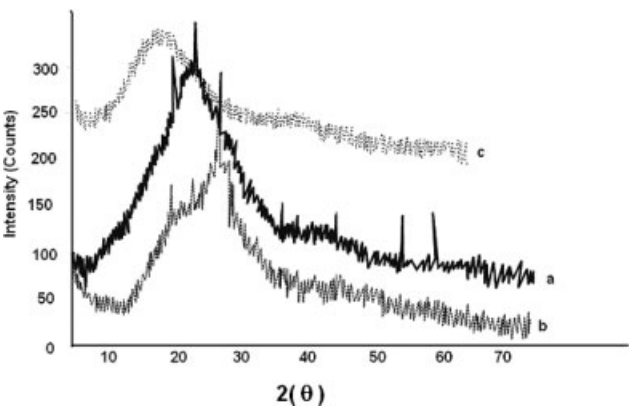

Figure 3 X-ray diffractograms of (a) PNA, (b) PNA-*co*-POT, and (c) PNA-*co*-PANI.

TABLE II
Characteristics of the X-Ray Diffraction Patterns

L (Å)	*d*-spacing (Å)	Polymer
1.466	4.7	PNA
1.475	4.9	PNA-*co*-PANI
1.32	3.6	PNA-*co*-POT

ing, calculated from angular positions of the reflections, is given in Table II, and from reflection broadening (2θ), the coherence length (*L*) of the crystalline order in the sample is calculated with the Scherrer formula:[19]

$$L = 0.9\lambda/2\theta\cos\theta$$

where λ is the wavelength of copper radiations (1.54 Å). Table II shows that there is an increase in the *d* spacing and *L* as aniline is added to the copolymer, whereas for PNA-*co*-POT, the *d*-spacing decreases along with *L*, and this may be due to the presence of a methyl group on the aromatic ring, which increases disorder and crystal size. For PNA-*co*-PANI, the increase in *L* between the chains is caused by greater order produced in the interchain separation within a crystalline region along the main copolymer chain, whereas the decrease in *L* for PNA-*co*-POT can be attributed to the amorphous and disordered alignment of the chains due to steric hindrance of the substituent methyl group.

Morphological analysis

The TEM image of PNA [Fig. 4(a)] shows spherically shaped globules having a high tendency to aggregate. The average size of the discrete globules was determined to be 30–50 nm in diameter. Such aggregation takes place during sample preparation for TEM when dispersions are evaporated on a carbon-coated copper grid. The size of the particles is strongly dependent on the dilution of the dispersion, and this supports the argument of aggregation happening during sample preparation and can be attributed to inefficient steric stabilization.

The TEM image of PNA-*co*-PANI [Fig. 4(b)] exhibits a dense distribution of discrete particles with little aggregation, the average size of the particles being 150 nm. The particles appear to be spherical. The well-organized particles lead to a more ordered morphology. The TEM micrograph of PNA-*co*-POT [Fig. 4(c)] shows discrete and somewhat elongated particles of the copolymer with an average size of 130 nm.

Unlike PNA, the particles of the copolymers show less tendency of aggregation.

Thermal analysis

The TGA thermogram of pure PNA (Fig. 5) shows a sluggish decomposition curve spreading from 180 to 620°C with two decomposition events. The first

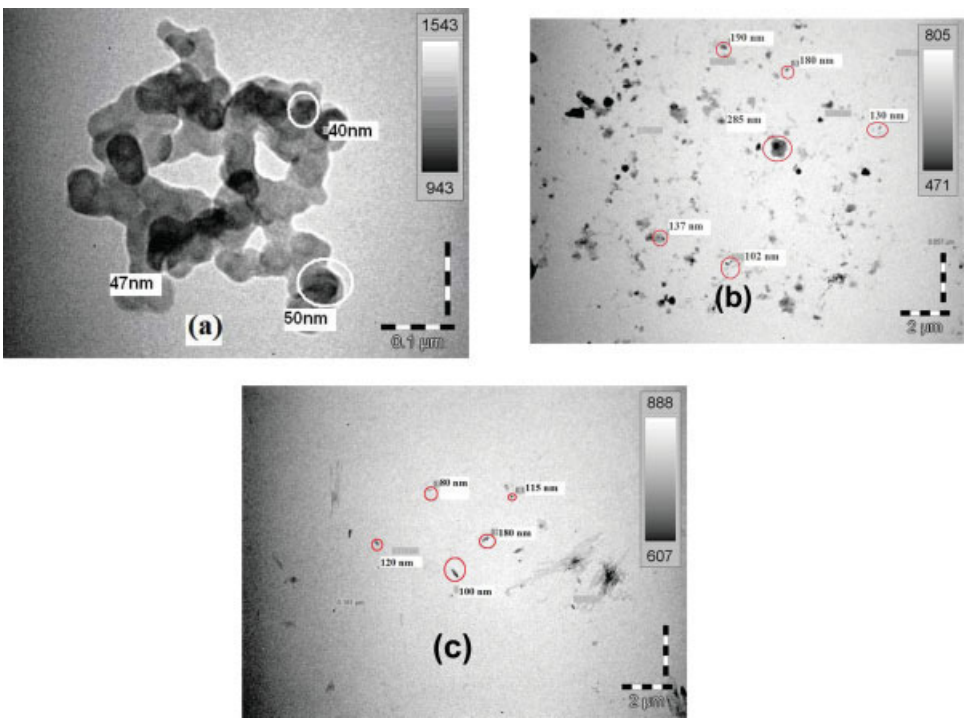

Figure 4 TEM images of (a) PNA, (b) PNA-*co*-PANI, and (c) PNA-*co*-POT. [Color figure can be viewed in the online issue, which is available at www.interscience.wiley.com.]

decomposition event is observed at 180°C, at which almost 10 wt % weight loss takes place. This may be attributed to the evaporation of the trapped solvent and other impurities such as the unreacted monomer and surfactant. Around 50 wt % loss is observed at 490°C in the second decomposition event, which is due to the degradation of the polymer. Almost 90% weight loss takes place at 720°C, leaving a residue of 10 wt %.

Compared to pure PNA, PNA-*co*-PANI (Fig. 5) shows decomposition behavior with a slower rate. The degradation temperature for 50 wt % decomposition increases significantly from 490 to 520°C, and this suggests extensive interchain linking and hydrogen bonding in this copolymer, whereas the TGA thermogram of PNA-*co*-POT (Fig. 5) shows a steep decomposition curve with a decrease in the 50 wt % decomposition temperature from 490°C for pristine PNA to 470°C.

It can be concluded that the thermal stability of PNA increases with the incorporation of aniline into the PNA backbone, whereas it decreases upon the incorporation of *o*-toluidine because of the steric hindrance, which is in agreement with the conformational structures of the homopolymer and copolymer.

Conductivity studies

The conductivity values of undoped and doped samples of PNA, PNA-*co*-PANI, and PNA-*co*-POT are given in Table III. The conductivity of the undoped sample of PNA was found to be 5.4×10^{-9} S/cm^{-1}. Doping of PNA with HCl and with I_2 led to a significant increase in the conductivity by 5 orders, that is, 8×10^{-4} and 7.1×10^{-4} S/cm^{-1}, respectively. The conductivity of the copolymers was found to be higher than that of the homopolymer. The conductivity for HCl- and I_2-doped PNA-*co*-PANI was found to be equal to 6.2×10^{-3} and 5.2×10^{-3} S/cm, respectively. The conductivity can be correlated to the number of charge carriers and the conjugation length along the polymer backbone. The conductivity of HCl- and I_2-doped PNA-*co*-POT was found to be 4.5×10^{-4} and 7.6×10^{-4} S/cm, respectively, and was lower than that of the homopolymer. The presence of aniline in the copolymer significantly enhanced the conductivity of PNA because higher conjugation led to greater transport of charge carriers. For PNA-*co*-POT, the presence of methyl substituents hindered charge transfer, and this caused a drop in the conductivity value.

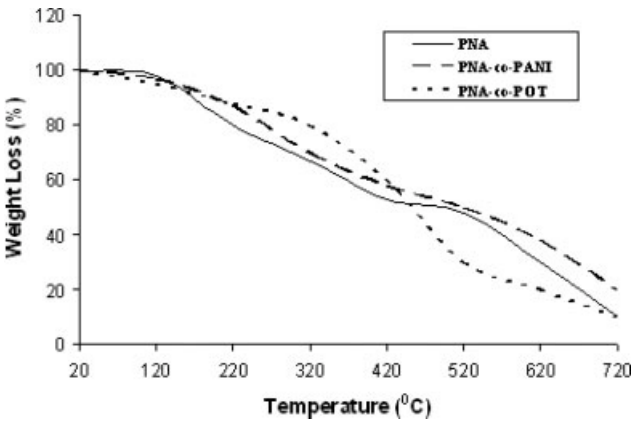

Figure 5 TGA thermograms of PNA and its copolymers.

TABLE III
Conductivity Values of PNA and Its Copolymers

Sample	Conductivity (S/cm)
PNA (undoped)	5.4×10^{-9}
PNA (HCl-doped)	8×10^{-4}
PNA (I_2-doped)	7.1×10^{-4}
PNA-*co*-PANI (undoped)	3.8×10^{-9}
PNA-*co*-PANI (HCl-doped)	6.2×10^{-3}
PNA-*co*-PANI (I_2-doped)	5.2×10^{-3}
PNA-*co*-POT (undoped)	4.3×10^{-9}
PNA-*co*-POT (HCl-doped)	4.5×10^{-4}
PNA-*co*-POT (I_2-doped)	7.6×10^{-4}

CONCLUSIONS

The effects of the comonomer type and polymerization conditions on conducting copolymers of PNA with *o*-toluidine and aniline synthesized with the inverse emulsion techniques were studied. FTIR and UV–vis spectra confirmed copolymerization. The particle sizes of the homopolymer and copolymers were in the nanoscale range. The particle size of PNA was lower than those of PNA-*co*-PANI and PNA-*co*-POT, the sizes being 50, 150, and 130 nm, respectively. PNA was found to be semicrystalline, PNA-*co*-PANI was partly crystalline, and PNA-*co*-POT was almost amorphous. PNA-*co*-PANI exhibited increased conductivity in comparison with PNA and PNA-*co*-POT. Copolymerization brought about a change in the chain conformation, particle size, particulate nature, and electrical conductivity. Another advantage of copolymerization was the formation of discrete and more or less agglomerated free particles, which resulted in a homogeneous material, the properties of which could be regulated by changes in the types of the comonomers in the feed.

References

1. Yang, Y.; Wan, M. J. Mater Chem 2002, 12, 897.
2. Borole, D. D.; Kapadi, U. R.; Mahulikar, P. P.; Hundiwale, D. G. Des Monom Polym 2004, 7, 45.
3. Dhawan, S. K.; Trivedi, D. C. Synth Met 1993, 60, 63.
4. Xu, L. G.; Ng, S. C.; Chan, H. S. O. Synth Met 2003, 123, 403.

5. Wei, Y.; Focke, W. W.; Ray, A.; MacDiarmid, A. G. J Phys Chem 1989, 93, 495.
6. Wei, Y.; Hariharan, R.; Patel, S. A. Macromolecules 1990, 23, 764.
7. Bergeron, J. Y.; Dao, L. H. Polym Commun 1991, 32, 403.
8. Umare, S. S.; Borkar, A. D.; Gupta, M. C. Bull Mater Sci 2002, 25, 235.
9. Langer, J. J. Synth Met 1990, 35, 301.
10. Porter, T. L.; Caple, G.; Lee, C. Y. Synth Met 1992, 46, 105.
11. Li, X.; Sun, C.; Wei, Z. Synth Met 2005, 155, 45.
12. Moon, D. K.; Osakada, K.; Maruyama, T.; Kubota, K.; Yamamoto, T. Macromolecules 1993, 26, 6992.
13. Schmitz, B. K.; Euler, W. B. J Electroanal Chem 1995, 399, 47.
14. Chung, C. Y.; Wen, T. C.; Gopalan, A. Mater Chem Phys 2001, 71, 148.
15. Huang, S. S.; Lin, H. G.; Yu, R. Q. Anal Chim Acta 1999, 262, 331.
16. Eramo, F. D.; Marioli, J. M.; Sereno, L. E. Electroanalysis 1999, 11, 481.
17. (a) Heeger, A. J. Angew Chem Int 2001, 40, 2591; (b) Cao, Y.; Smith, P.; Heeger, A. J. Synth Met 1992, 48, 91.
18. Marianovic, G. C.; Marjanovic, B.; Stamenkovic, V.; Vitnik, Z.; Antiv, V.; Juranic, I. J. Serb Chem Soc 2002, 67, 867.
19. Borkar, A. D.; Gupta, M. C.; Umare, S. S. Polym Plast Technol Eng 2001, 40, 225.
20. Huang, J.; Virji, S.; Weiller, B. H.; Kaner, R. B. J Am Chem Soc 2003, 125, 314.
21. Zhang, X.; Roch, C. Y. K.; Jose, A.; Manohar, S. K. Synth Met 2004, 145, 23.
22. Huang, W. S.; MacDarmid, A. G. Polymers 1993, 34, 1833.
23. Xia, Y.; Weisinger, G. M.; MacDiarmid, A. G. Chem Mater 1995, 7, 443.
24. Laska, J.; Widlarz, J. Polymer 2005, 40, 1485.
25. Boyer, M. I.; Quillard, S.; Rebourt, E.; Louaran, G.; Buisson, J. P.; Monkman, A.; Lefrant, S. J Phys B 1998, 102, 7382.
26. Pomfret, S. J.; Rebourt, E.; Monkman, A. P. Synth Met 1996, 76, 19.